

# A Cross-Stacked Radiating Antenna With Enhanced Scanning Performance for Digital Beamforming Multifunction Phased-Array Radars

José D. Díaz<sup>1</sup>, *Student Member, IEEE*, Jorge L. Salazar-Cerreno, *Senior Member, IEEE*,  
 Javier A. Ortíz<sup>2</sup>, *Student Member, IEEE*, Nafati A. Aboserwal<sup>3</sup>, *Member, IEEE*,  
 Rodrigo M. Lebrón, *Student Member, IEEE*, Caleb Fulton<sup>4</sup>, *Senior Member, IEEE*,  
 and Robert D. Palmer, *Fellow, IEEE*

**Abstract**—This contribution presents the results of a dual-polarized radiating element designed to achieve low cross-polarization (lower than  $-40$  dB measured for the E- and H-plane, at least  $-30$  dB in the D-plane based on simulations) and large fractional bandwidth (18%) over wide scanning angles ( $\pm 60^\circ$ ). The proposed design includes multiple features that enable high isolation between ports, reduction of spurious radiation, highly symmetrical radiated fields, and suppression of diffracted fields between contiguous subarray gaps. To verify the polarimetric requirements for a weather radar, simulated and measured results, including electronic scanning of the array and embedded element patterns of the antenna, are shown.

**Index Terms**—Aperture-coupled, cross-patch antenna, digital beamforming, dual polarized, microstrip patch antenna, multifunction phased-array radar (MPAR), phased-array radar, stacked patch, wide angle, wideband.

## I. INTRODUCTION

THE multifunction phased-array radar (MPAR) initiative presented an opportunity for the design of high-performance antenna elements that are capable of atmospheric interrogation and aircraft surveillance. Some antenna architectures have been proposed to comply with the dual-polarization demand [1]–[7], but a little has been reported compiling weather requirements and design considerations for MPAR antennas. Depending on the architecture of the array, the performance of these elements will be exposed to different scenarios that drive the performance of the whole array. Series-fed antenna architectures [1], [2] allow for a reduced number of Tx and Rx channels, while the complexity in the design of the antenna is increased. The same is true for overlapped subarrays [3], for which beamforming architectures present another challenge independent of the

design of the antenna element. These techniques are the examples of experimental MPAR beamforming concepts that are continuing to be tested today to satisfy the weather and aircraft surveillance needs of this mission.

As a part of this initiative, the Advanced Radar Research Center proposed a fully digital, element-level digitization MPAR line replaceable unit [4] that allows for highly flexible fast scanning strategies and beamforming techniques [8]. Element-level control, in this context, is the ability to operate a dual-polarized antenna element with individual channels for both H- and V-polarization. The design of such array front ends is considerably easier than any other antenna architecture, while significantly more challenging for the array back end. From an antenna designer's perspective, the performance of a big array with this level of control will be determined by the embedded antenna element characteristics. For example, the cross-polarization level in an array where all the elements are identical is defined by the embedded element pattern and the array factor [9]. Moreover, the embedded element pattern is also related to the active impedance of the array [10], which defines the efficiency of the antenna as it scans. These features are important to understand, since they describe the performance of the array in terms of the antenna element from which it is designed.

Now that the importance of the antenna element is established, the MPAR requirements will dictate the selection of the antenna. Bandwidth, isolation, cross-polarization, scanning performance, and manufacture tolerances are some of the most crucial factors that must be considered in the selection of the element. Co-polar patterns with differences of 0.1 dB between polarizations and cross-polarization levels lower than  $-40$  dB are required within a scanning range of  $\pm 45^\circ$ . These requirements are to date some of the most constraining for dual-polarized phased array radars [11], [12].

Numerous techniques to design and improve the performance of microstrip patch antenna elements have been discussed [9], [13]–[15]. These articles comprehensively cover different aspects of the design of microstrip patch antennas and provide guidelines for their use in phased arrays. It is in the interest of this paper to review some of the methods discussed

Manuscript received March 1, 2017; revised April 12, 2018; accepted April 21, 2018. Date of publication August 1, 2018; date of current version October 4, 2018. This work was supported by the NOAA's National Severe Storms Laboratory under the CIMMS Cooperative Agreement NA11OAR4320072. (Corresponding author: José D. Díaz.)

The authors are with the Advanced Radar Research Center, Department of Electrical and Computer Engineering, The University of Oklahoma, Norman, OK 73019 USA (e-mail: salazar@ou.edu).

Color versions of one or more of the figures in this paper are available online at <http://ieeexplore.ieee.org>.

Digital Object Identifier 10.1109/TAP.2018.2862252

0018-926X © 2018 IEEE. Personal use is permitted, but republication/redistribution requires IEEE permission.  
 See [http://www.ieee.org/publications\\_standards/publications/rights/index.html](http://www.ieee.org/publications_standards/publications/rights/index.html) for more information.

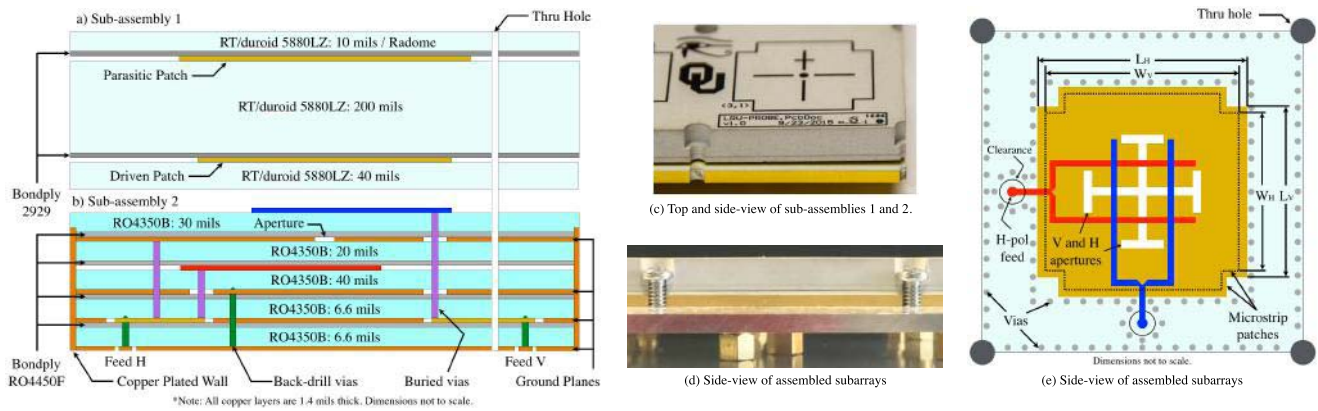


Fig. 1. (a) Stack-up of the radiator assembly for the subarrays with the materials and heights used for the design. (b) Stack-up of the feeding network assembly for the subarrays with the materials and heights used for the design. (c) Top and side views of the manufactured subarrays. (d) Side view of the assembled manufactured subarrays. (e) Top view of the antenna element.

in previous contributions while narrowing the techniques that can be applied to comply with antenna weather requirements for the MPAR initiative. A dual, linearly polarized aperture-coupled, cross-stacked microstrip patch radiating element is presented and proves to overcome scanning losses while showing low cross-polarization through the whole scanning range of interest.

In Section II, a discussion of current trends in the design tradeoffs of high-performance radiating elements is developed with enfaces to overcome bandwidth, cross-polarization, and manufacturability issues. Section III discusses all applied techniques to design the antenna element and its array including simulated results. Section IV of this contribution presents the performance of the embedded antenna element and the measured scanning capabilities of the array in far-field and near-field ranges. In Section V, the most important contributions and achievements in the antenna community resulting from this paper for the MPAR mission are detailed.

## II. ANTENNA DESIGN TRADEOFFS

The goals for the performance of the antenna element were first presented in [4]. In that contribution, the simulated results for the antenna element on a  $\lambda_o/2$  ground plane included active reflection coefficients, cross-polarization levels in the principal planes, and preliminary antenna pattern measurements at the array level. In Sections II-A–II-C, we discuss which factors were involved in the selection of the antenna architecture that provided these results.

### A. Bandwidth

One of the main drawbacks of using microstrip patch antennas is their limited impedance bandwidth [13]–[15]. This limitation is even more evident in phased-array antennas when sometimes a need for different feeding networks for specific elements can result in a reduction of the impedance bandwidth of the array. Using a thick material with a low dielectric constant could potentially overcome the bandwidth difficulty. However, surface waves can propagate as the thickness of the dielectric is increased [15]. In a case where a bandwidth

of 10% is expected for a material with a dielectric constant of 2.2, the resultant thickness is approximately  $0.07\lambda_o$  for a single patch, according to [16]. This is a clear constraint for practical microstrip patch antenna arrays that are designed for low frequencies, given that these thicknesses typically exceed manufacturing industry standards. One way to avoid the use of thick materials, which improves the bandwidth, is using multisection matching networks with the antenna element. However, size constraints of the unit cell (typically  $0.5\lambda_o$ ) make multisection matching networks difficult to apply in planar arrays [16]. Another approach to improve the bandwidth is to use the stacked patch configuration, which offers an increased aperture efficiency of the antenna when compared with a single patch element [17]. This technique allows for a reduction in the dielectric thickness required to achieve the same bandwidth when compared with a single patch antenna. Section III presents the design approach that combined several techniques including the cross-stacked patch, as shown in Fig. 1. This approach enabled 18% impedance bandwidth for the presented antenna element.

### B. Isolation and Cross-Polarization

The isolation and cross-polarization levels of dual-polarized microstrip patch antennas are determined by unwanted excited modes, which are related to the physical characteristics of the radiator such as dielectric thickness, width, length, and feeding network of the patch [18], [19]. In terms of today's radar design requirements, cross-polarization levels for simultaneous and alternate transmission are on the order of  $-40$  and  $-20$  dB, corresponding to an accuracy in the differential reflectivity below 0.2 dB [11]. Techniques for arrays and elements have been discussed in the literature to suppress cross-polarized radiation. At the array level, mirroring of antennas lowers the overall cross-polarization of the array due to the cancelation of fields coming from neighboring elements [20].

At the element, balanced probe-fed microstrip patches have reached the cross-polarization levels of  $-30$  dB with a significant increase in complexity due to the hybrid feeding network needed to produce the proper phase between

the excitations [5]. Moreover, this technique requires the connection of two or four probes directly soldered to the microstrip patch, and in an array with thousands of elements, the large number of solder joints could reduce the reliability of the system [15]. Another approach to suppress cross-polarization on the antenna element is defective ground structures (DGS) [21], [22]. DGS had proved to reduce cross-polarization levels in microstrip patch antennas to the same level of the balanced feed configuration. It is important to note that DGS are often used for probe-fed or in-set fed linearly polarized microstrip patch antennas.

Considering noncontacting feeds, aperture-coupled microstrip antennas generally offer a more robust design, because their construction lacks soldered feed pins [23]. An aperture is located on a ground plane that separates both vertical and horizontal polarizations. Each feeding network couples to the aperture, while the aperture then couples the energy to the driven patch. A cross-sectional view of this mechanism using stacked patches is shown in Fig. 1(a) and (b). This technique allows for high isolation between ports, which is inherently related to the cross-polarization level [24]. On the downside, the construction of this configuration is difficult and the back-lobe radiation is higher than the traditional probe-fed patch due to the energy coming from the slot [25]. In order to reduce the radiation that comes from the slot, a feeding network based on striplines with a backing ground plane could be used for one of the polarizations, as shown in Fig. 1(a) and (b). In terms of cross-polarization, this technique shows better performance than other feeding methods when the apertures are designed to keep cross-polarized radiation away from broadside [26]. In Section III, it is shown that isolation levels below  $-48$  dB are possible in the element while the scanned cross-polarization can be maintained below  $-40$  dB.

### C. Manufacturability

The performance against the temperature of the antenna should be as constant as possible to avoid uncertainty in the calibration of the array. Besides having a low dielectric constant, the materials on a stacked patch configuration should have similar thermal expansion coefficients (TECs) to prevent misalignment of the radiators during manufacturing or operation of the array (see Table I). Using different materials for multilayer structures (i.e., with different TECs) is not encouraged due to various rates of expansion that could occur across surfaces. Most active phased-array antennas for radar applications, especially the long-range radars, require transmitting peak power in the order of several kilowatts. Power dissipation in the antenna front end can easily delaminate or warp the multilayer structure degrading the overall performance of the array. In some cases, warping of the multilayer antenna array can occur during the manufacturing process. To avoid this warping is recommended the use of balance multilayer structures. Unfortunately, using balance stack-up is not always good for high RF performance. To minimize this issue, the proposed antenna array was constructed by stacking two independent assemblies, as shown in Fig. 1(a) and (b).

TABLE I  
ANTENNA MATERIALS USED FOR THE DESIGN

Materials	TEC: X, Y, Z	$\epsilon_r$	Dissipation Factor
RO4350B	10, 12, 32	3.66	0.0031
RO4450F	19, 17, 50	3.52	0.0040
2929 Bondply	50, 50, 50	2.94	0.0030
RT/duroid 5880LZ	44, 43, 41.5	1.96	0.0019

With this approach, lamination cycles for each subassembly are reduced independently when compared with a single assembly. To reach the interconnection of the assemblies and the flatness of the mounted array, screws around the elements are placed and tightened as seen in Fig. 1(c) and (d).

## III. DESIGN APPROACH

### A. Antenna and Feeding Network

After reviewing different types of feeding networks, a non-contact feed network was chosen. A noncontact feed network allows for high isolation between polarizations, and thus, channel interactions are suppressed. The feeding network discussed in [27] allows for both the polarizations to coexist while being separated by a ground plane. The results of this separation is the exceptional isolation between polarizations in the order of  $-40$  dB. Moreover, this feeding network allows for having symmetrical apertures on the ground plane. Symmetry is important at the element level in order to cancel near-field interactions that might increase the cross-polarization at the array level and to maintain similar performance for both H- and V-polarization.

To overcome the bandwidth difficulty, a stacked patch configuration was adopted. The combination of the previously mentioned feeding network with the stacked patch is presented in [28]. To optimize the model, guidelines discussed in [29] were followed, because they apply to dual-polarized antennas. In this design, the excitation of the aperture as a resonant source to increase the bandwidth was not employed. In other words, the bandwidth enhancement was only due to the coupling between the cross-stacked microstrip patches. This consideration is essential, given that the radiation coming from the aperture is not contributing to the radiated fields in the desired bandwidth, which have the potential to jeopardize cross-polarization levels.

For manufacturing purposes, the radiators and the feeding network were separated into two different assemblies to prevent them from delamination and bending. The radiator assembly consists of two conducting layers and a radome of RT/duroid 5880LZ bonded with Bondply 2929. The low permittivity values of the dielectrics in the radiator's assembly ensure higher bandwidths. The presence of the radome has a little to no effect on the radiated fields and allows for marking the layer with a cross pattern that identifies the center of the antenna element as seen in Fig. 1(c). This center is going to be recognized by a high-definition camera for calibration purposes [30].

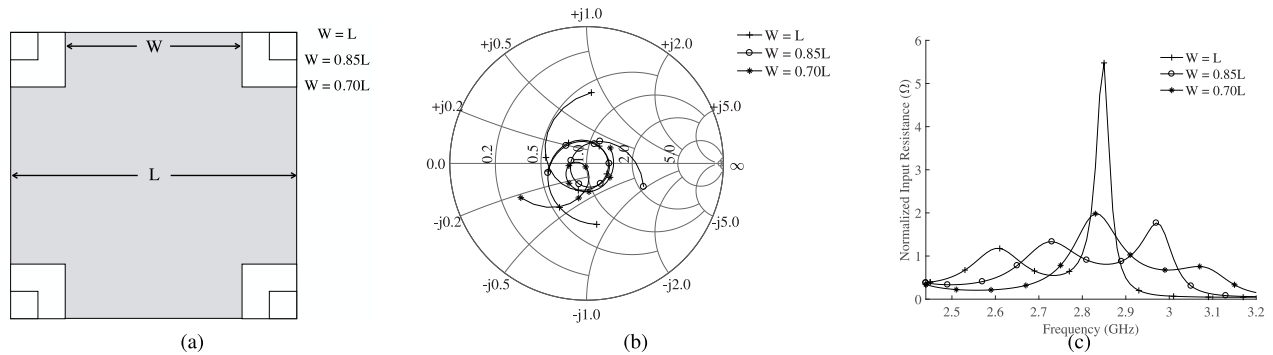


Fig. 2. (a) Top view of the cross-patch antenna element with variations in the width:  $W = L$ ,  $W = 0.85L$ , and  $W = 0.70L$ . (b) Normalized ( $50\ \Omega$ ) real part of the input impedance across frequencies in the cross-patch antenna element as the ratio of  $W/L$  decreases. (c) Loci of the normalized input impedance as the ratio of  $W/L$  decreases.

The feeding network assembly is made out of six conducting layers bonded with RO4450F. A more detailed description of the materials used for the array is shown in Table I. The stack-up for the array is shown in Fig. 1(a) and (b). Note that the feeding network assembly uses RO4450F, because it has similar electrical properties to RO4350B. Fig 1(c) and (d) shows the side view of manufactured assemblies. It can be seen that when both the assemblies are connected, the bend that is present in the radiators and feeding network assemblies disappears because of the screws. Blind plated vias were placed around the periphery of the element below the aperture ground, as shown in Fig. 1(e), to minimize the interaction between the apertures and the feeding networks. To further decrease the presence of any spurious modes, blind plated vias were also put around the H- and V-feeds. To maximize the conductivity and isolate the effects of neighboring subarrays, a 10 mil copper-plated wall was included in the feeding network assembly, as shown in Fig. 1(b)–(d), which matches the same height of the blind vias.

Until this point, the focus of the discussion has been in the design of the feeding network and the materials employed in the antenna stack-up, yet the geometry of the radiator also influences the cross-polarization and the bandwidth. In general, rectangular microstrip patches exhibit higher bandwidths when the width is greater than the length [16]; however, this geometry does not allow dual-polarization to occur in the microstrip patch. To produce the dual-polarization mode operation, a square patch antenna is commonly used. One important limitation of square patch antennas is its high-impedance sensitivity and its cross-polarization due to the excitation of higher order modes as a function of the feed position [18], [19], [31]. In this design, the cross-patch ratio ( $W/L$ ) was used to achieve the desired coupling in the antenna element. The features of this treatment are shown in Fig. 2(a)–(c). As  $W/L$  decreases with  $L$  constant, the impedance loci rotate clockwise [see Fig. 2(b)], indicating an increase in the inductance due to the narrowing of the patch. Concurrently, the operational frequencies of the patches shift higher, as shown in Fig. 2(c). This result is expected, given that the radiator becomes electrically smaller than a full square patch. Using the cross-patch geometry, the cross-polarization in the antenna is enhanced and there

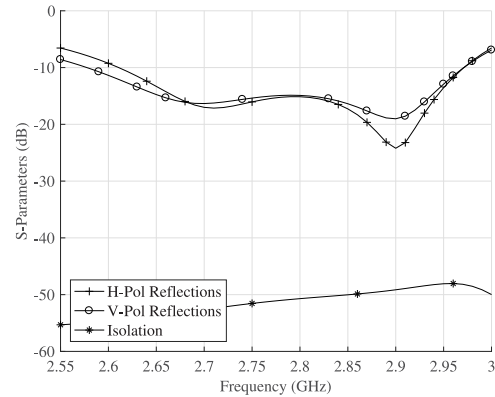


Fig. 3. Simulated isolated antenna element reflections and isolation between polarizations using HFSS.

is a little effect on the bandwidth when compared with the square geometry. The S-parameters of the proposed antenna element are presented in Fig. 3. The overlapped bandwidth between the polarizations is roughly 400 MHz or 18% (lower than  $-10$  dB), and the isolation between the ports' peaks at 2.97 GHz with a value of  $-48$  dB when implementing the cross-stacked patch antenna and the aperture coupling technique.

### B. Antenna Array

In general, there are two factors involved in scanning performance, the size of the unit cell to minimize the possibility of grating lobes, and surface waves that could allow scan blindness. To avoid the presence of grating lobes in a phased-array antenna, the spacing between elements is selected to be lower than  $\lambda_o/2$ . With a center frequency of 2.8 GHz, the size of a unit cell for a square lattice array is 53.55 mm that corresponds to  $\lambda_o/2$ ; however, the designed array has a spacing of 50.8 mm. A set of simultaneous transcendental equations [32] were used to estimate the boundaries established by the grating lobe diagram, given the corresponding spacing of the designed array and the radiators' assembly properties. An average weighted permittivity that includes all layers in the radiator's assembly and the dielectric of the V-pol transmission line

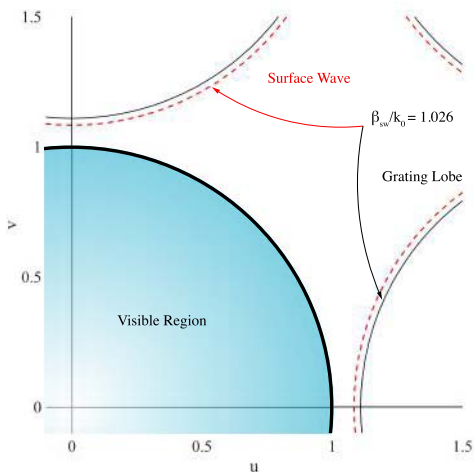


Fig. 4. Grating lobe diagram using a spacing of  $d_x = d_y = 50.8$  mm, an averaged permittivity of 2.14 that includes all dielectrics above the aperture ground plane from Fig. 1(a), and an operational frequency of 2.8 GHz.

TABLE II  
SCANNING PERFORMANCE

Parameter	Frequency (GHz)		
	2.7	2.8	2.9
Element spacing ( $d_x, d_y$ )	$0.457 \lambda_o$	$0.474 \lambda_o$	$0.491 \lambda_o$
Surf. waves propag. const. ( $\beta_{sw}/k_0$ )	1.0254	1.0256	1.0285
Scanning range (E-,H and D-planes)	$\pm 45^\circ$	$\pm 45^\circ$	$\pm 45^\circ$
Scan blindness in the visible region	none	none	none

(i.e., the dielectric above the aperture) was calculated to be 2.14, with an overall height of 280 mils or  $0.0664 \lambda_o$ .

Fig. 4 shows the grating lobe diagram that illustrates the impact of the surface waves in the visible region at the center frequency. It can be seen that the surface-wave contribution added to the diagram yields no gratings lobes in the visible region. The analysis was extended to other frequencies of interest in the antenna and the results are shown in Table II. It can be seen that for the highest operational frequency, the unit cell size is less than  $\lambda_o/2$ . Higher order modes of surface waves are not excited in the proposed antenna array, while parallel plate modes were mitigated using vias in the transmission line subassembly [see Fig. 1(b)]. Infinite-array numerical simulations of the antenna unit cell in Ansys high-frequency structure simulator (HFSS) were used to validate the overall scanning performance of the array. Fig. 5 shows the active reflection coefficient for the antenna element for E-, D-, and H-planes and both the polarizations at 2.8 GHz. No scan blindness was found in the principal planes for both the polarizations. Fig. 6 shows the gain loss of the antenna using the active reflection coefficient data from the results presented in Fig. 5. It can be seen that less than 0.4 dB loss is expected when the antenna scans to  $60^\circ$ .

To minimize the effects of cross-polarization contamination due to the exposed feeding network (V-polarization), a mirroring technique at the array level was adopted [20]. The method enables the cancelation of near-field interactions between the feed networks exposed above the aperture ground plane. Once designed, the antenna element was expanded into a  $2 \times 4$  unit cell and the  $8 \times 8$  array was achieved using the

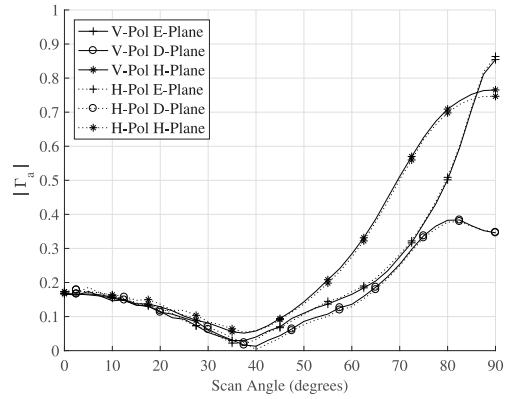


Fig. 5. Simulated active reflection coefficient for the antenna using HFSS at 2.8 GHz.

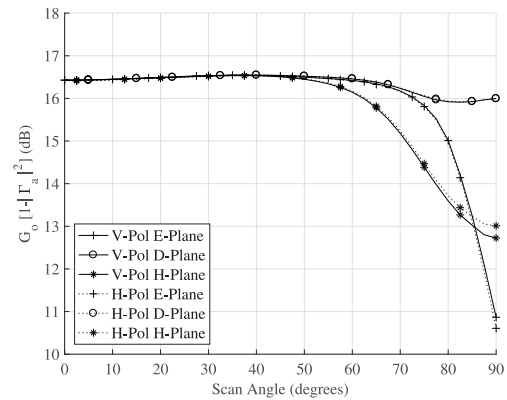


Fig. 6. Simulated gain loss for a  $2 \times 8$  antenna array using the active reflection coefficient results from Fig. 5.

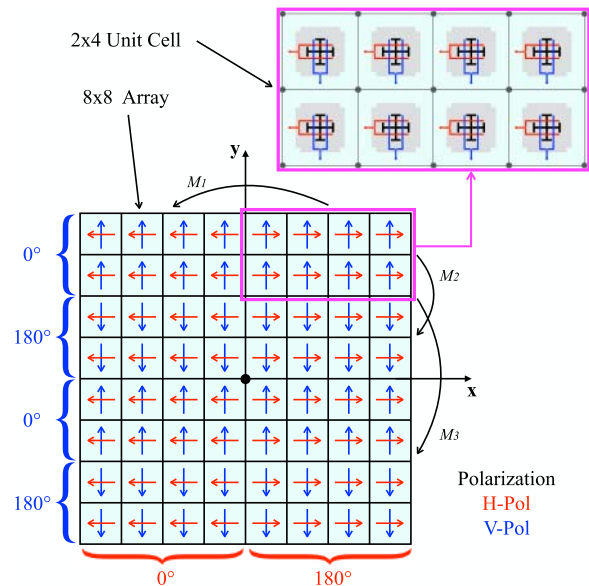


Fig. 7. Resultant polarization of the elements on the  $8 \times 8$  array when duplicating the  $2 \times 4$  unit cell using mirror operations.  $M_1$ ,  $M_2$ , and  $M_3$  refer to the applied mirror operations on the  $2 \times 4$  unit cell parallel to x-, y-, and y-axes, respectively.

mirror operations shown in Fig. 7. It can be seen that the V-polarization is physically  $180^\circ$  out of phase every two rows in the  $8 \times 8$  array while the H-polarization is mirrored along the y-axis.

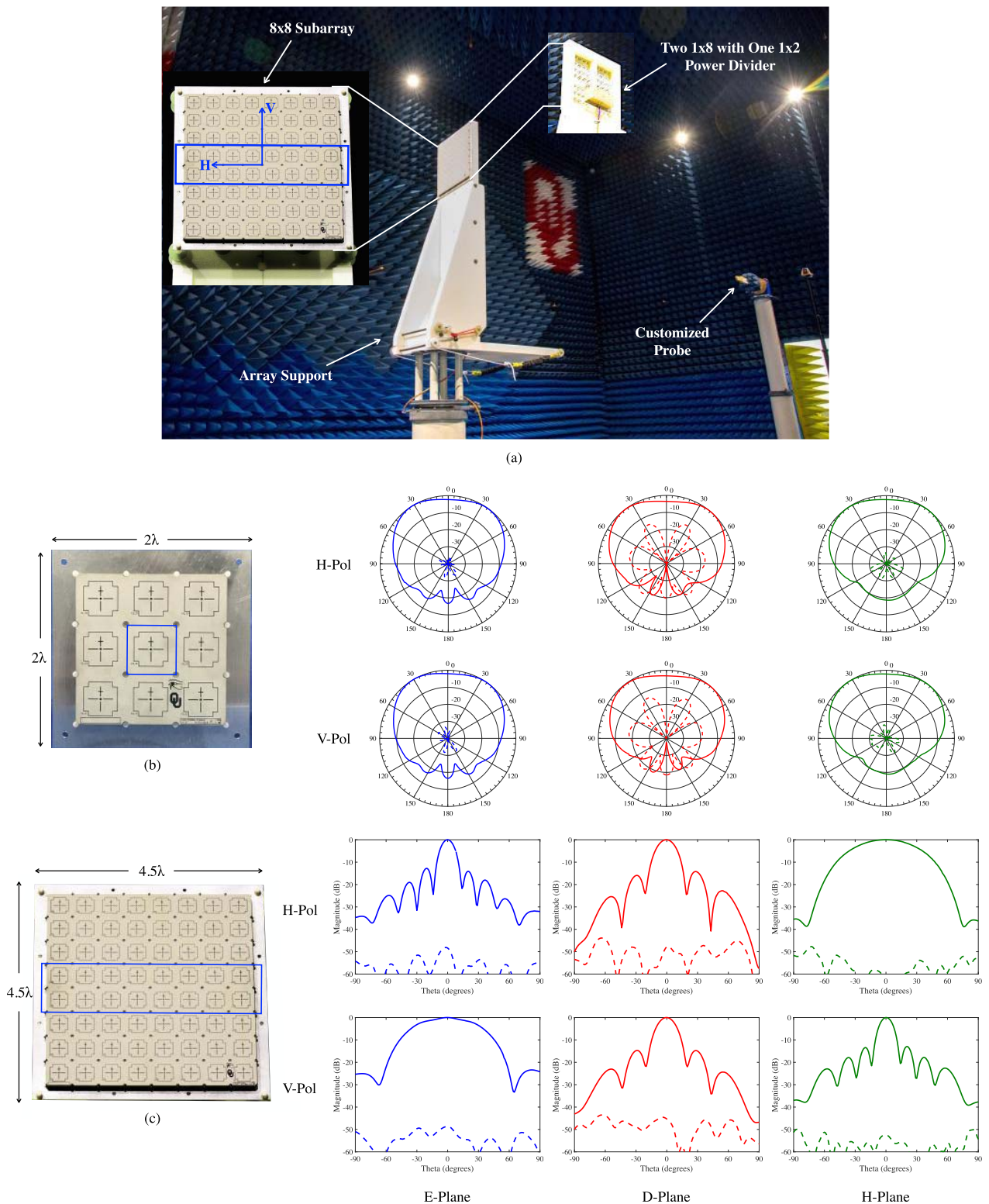


Fig. 8. (a) Far-field chamber used for the setup and measurements of the antenna subarrays. (b) Measured radiation patterns at 3.0 GHz for H- and V-polarizations on the center element of the  $3 \times 3$  subarray mounted on a ground plane that protrudes  $\lambda_o/2$  from the antenna. (c) Measured radiation patterns at 3.0 GHz for H- and V-polarizations on the  $8 \times 8$  subarray mounted on a ground plane that protrudes  $\lambda_o/2$  from the antenna. Solid and dashed lines refer to co- and cross-polarization.

#### IV. RESULTS

In order to simplify the measurements of the radiation patterns of the array and the antenna element, the authors

used polarization based on Ludwig’s third definition. However, to accurately describe the cross-polarization away from the principal planes, Ludwig’s second definition should be used,

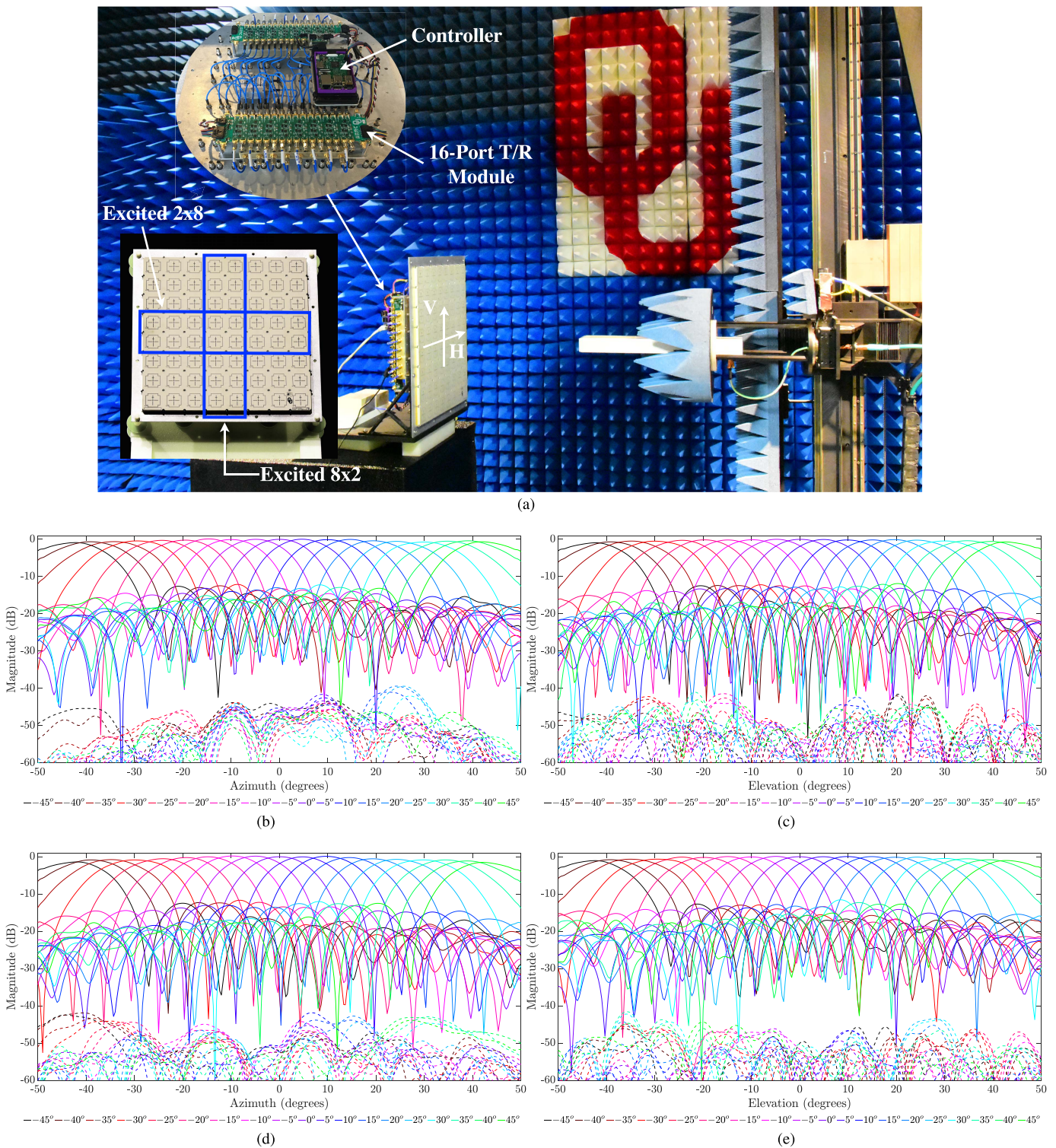


Fig. 9. (a) Near-field chamber setup for electronically scanned radiation patterns of an array  $2 \times 8$  elements embedded in an array of  $8 \times 8$  elements at 3 GHz. (b) and (d) Measured radiation patterns of  $2 \times 8$  array (for H- and V-polarizations) in the azimuth plane. (c) and (e) Measured radiation patterns of  $8 \times 2$  array (for H- and V-polarizations) in the elevation plane. Solid and dashed lines refer to co- and cross-polarization.

since microstrip patch antennas are not Huygen sources [33]. In this section, we discuss the measured results of antenna patterns (embedded element and array patterns) performed in a far-field and near-field anechoic chambers at the Radar Innovation Laboratory at The University of Oklahoma (OU).

Measurements for the patterns were first conducted in a far-field range using a customized NSI-RF-WR284 waveguide probe that operates in a frequency range from 2.6 to 3.95 GHz. A customized fixture [see Fig. 8(a)] constructed of high-performance Rohacell 110 IG/A with

$\epsilon_r = 1.12$  was used to support the array on a pedestal. This feature minimized reflections and disruption of patterns on the specular region of the far-field chamber. The antennas were attached to a solid aluminum plate that extended 1 in  $[(1/2)\lambda_0]$  from the border of the array, and the patterns were obtained at 3.0 GHz. As an effort to differentiate between the cross-polarization of the antenna element and the  $8 \times 8$  array, measurements of the center element on a  $3 \times 3$  array were performed and results are shown in Fig. 8(b). It can be seen that highly symmetrical co-polarizations were achieved for both H- and V-polarizations, and in terms of cross-pol, less than  $-34$  dB for the E-planes, better than  $-32$  dB for the H-planes, and about  $-13$  dB for the D-planes were measured.

For the array patterns, measurements for both the polarizations were taken while exciting the two middle rows on the  $8 \times 8$  array. To create the  $2 \times 8$  array pattern, two  $8 \times 1$  power combiners are used and connected with coaxial cables. In addition, phase shifters were added in the elements that were physically offset  $180^\circ$  due to antenna mirroring. Fig. 8(c) shows the measured co- and cross-polarization patterns using Ludwig's third definition. It can be seen that at broadside, the cross-polarization level is below  $-45$  dB for both the polarizations in the measured planes from  $\pm 45^\circ$  in azimuth. Even though the cross-polarization is close to the values obtained in simulations, the null of the antenna pattern are not well defined. This can be attributed to phase errors induced by the power combiners, cables, and the short distance (20% shorter than the actual far-field estimation) between the antenna array and the probe that does not satisfy the minimum distance required for far-field measurement.

In order to obtain the scanning performance of the antenna array and validate the measurements of the far-field range, a 16-channel board that contains digital phase shifter and attenuators was designed and fabricated. Fig. 9(a) shows the active array antenna setup at the OU near-field range, the T/R module board, the control board, and the measured scanned performance of the antenna array using the  $2 \times 8$  and  $8 \times 2$  configurations for H- and V-polarizations. Measurements were obtained every  $5^\circ$  in a scanning range of  $\pm 45^\circ$  for both the polarizations in the azimuth and elevation planes. To control the phase of the antennas, 6 bit serial control phase shifter and attenuator cards were made with a resolution of  $5.625^\circ$  and 0.5 dB for each element. A calibration algorithm was performed to remove the amplitude and phase inaccuracies between channels. Fig. 9(a) shows the antenna setup in the near-field chamber. Fig. 9(b) and (c) shows the two excited rows and the two excited columns co- and cross-polarization patterns [Fig. 9(d) and (e)] of the scanned array every  $5^\circ$ . It can be seen that the cross-polarization for all cases is roughly below  $-40$  dB for both the polarizations in the principal planes. At the time of publication, the resources for scanning the array in the D-plane were not available. For this reason, the scanned cross-polarization of the array was based on a HFSS domain decomposition method simulation that did not include the rotation of the elements in the array. The results of this simulation predict cross-polarization below  $-30$  dB for both the polarizations when scanning to  $\theta_0 = 45^\circ$  and  $\phi_0 = 45^\circ$ .

## V. CONCLUSION

The use of multiple techniques for improving the performance of an antenna element that could satisfy today's requirements for phased array weather radars was presented. A new coupling mechanism, the cross-patch ratio, was discussed and the results show how this parameter could help to achieve the required coupling on an aperture-coupled patch antenna. Measured scanning results in a far-field range for two rows and eight columns on an  $8 \times 8$  array were presented at broadside, and the results show cross-polarization levels below  $-45$  dB. To corroborate the far-field measurements, near-field measurements were performed and the results show the same cross-polarization at broadside, while a scanning cross-polarization of  $-40$  dB in the principal planes. As the number of elements increases, the authors expect that inaccuracies or phase differences in the cross-polarized radiation coming from the elements will further lower scanning cross-polarization. In summary, the authors have presented an optimized antenna element for MPAR purposes capable of achieving the bandwidth, isolation, scanning, and cross-polarization requirements for the MPAR mission.

## ACKNOWLEDGMENT

The authors would like to thank J. Christian and R. Kelley for their contributions in constructing the fixture used to measure the antennas. They would like to thank R. Kelley for assisting in the development of the manufacturing files of the subarrays. They would also like to thank A. Mancini, S. Duthoit, B. Brown, K. Constien, D. Hayes, and T. Brachtenbach for their help in the measurements.

## REFERENCES

- [1] J. L. Salazar, E. J. Knapp, and D. J. McLaughlin, "Dual-polarization performance of the phase-tilt antenna array in a CASA dense network radar," in *Proc. IEEE Int. Geosci. Remote Sens. Symp.*, Jul. 2010, pp. 3470–3473.
- [2] S. Karimkashi and G. Zhang, "A dual-polarized series-fed microstrip antenna array with very high polarization purity for weather measurements," *IEEE Trans. Antennas Propag.*, vol. 61, no. 10, pp. 5315–5319, Oct. 2013.
- [3] J. Herd and S. Duffy, "Overlapped digital subarray architecture for multiple beam phased array radar," in *Proc. 5th Eur. Conf. Antennas Propag. (EUCAP)*, Apr. 2011, pp. 3027–3030.
- [4] J. D. Díaz *et al.*, "A dual-polarized cross-stacked patch antenna with wide-angle and low cross-polarization for fully digital multifunction phased array radars," in *Proc. 5th Int. Symp. Phased Array Syst. Technol.*, Boston, MA, USA, Oct. 2016, pp. 1–4.
- [5] C. Fulton and W. Chappell, "A dual-polarized patch antenna for weather radar applications," in *Proc. IEEE Int. Conf. Microw., Commun., Antennas Electron. Syst. (COMCAS)*, vol. 2, Nov. 2011, pp. 1–5.
- [6] J. Salazar-Cerreno, E. Loew, P.-S. Tsai, J. Vivekanandan, W.-C. Lee, and V. Chandrasekar, "Design and development of a 2-D electronically scanned, dual-polarization, line replaceable unit (LRU) for airborne phased array radar for atmospheric research," in *Proc. 36th Int. Conf. Radar Meteorol.*, vol. 64, 2013, pp. 1–6.
- [7] J. L. S. Cerreno, "Dual-polarized radiating patch antenna," U.S. Patent 20160079672 A1, Mar. 17, 2016.
- [8] M. C. Leifer, V. Chandrasekar, and E. Perl, "Dual polarized array approaches for MPAR air traffic and weather radar applications," in *Proc. IEEE Int. Symp. Phased Array Syst. Technol.*, Oct. 2013, pp. 485–489.
- [9] D. M. Pozar and B. Kaufman, "Design considerations for low sidelobe microstrip arrays," *IEEE Trans. Antennas Propag.*, vol. 38, no. 8, pp. 1176–1185, Aug. 1990.

- [10] R. J. Mailloux, *Phased Array Antenna Handbook*. Norwood, MA, USA: Artech House, 2005.
- [11] Y. Wang and V. Chandrasekar, "Polarization isolation requirements for linear dual-polarization weather radar in simultaneous transmission mode of operation," *IEEE Trans. Geosci. Remote Sens.*, vol. 44, no. 8, pp. 2019–2028, Aug. 2006.
- [12] D. S. Zrnic and R. J. Doviak, "System requirements for phased array weather radar," NOAA/NSSL, Norman, OK, USA, Tech. Rep. 24pp, 2005.
- [13] K. Carver and J. Mink, "Microstrip antenna technology," *IEEE Trans. Antennas Propag.*, vol. AP-29, no. 1, pp. 2–24, Jan. 1981.
- [14] K. C. Gupta, "Broadbanding techniques for microstrip patch antennas—A review," Dept. Elect. Comput. Eng., Univ. Colorado, Denver, CO, USA, Tech. Rep. 98, 1988.
- [15] D. M. Pozar, "Microstrip antennas," *Proc. IEEE*, vol. 80, no. 1, pp. 79–91, Jan. 1992.
- [16] D. Pozar, "A review of bandwidth enhancement techniques for microstrip antennas," in *Microstrip Antennas: The Analysis and Design of Microstrip Antennas and Arrays*, D. M. Pozar and D. H. Schaubert, Eds. Hoboken, NJ, USA: Wiley, 1995, ch. 4, pp. 157–166.
- [17] A. Sabban, "A new broadband stacked two-layer microstrip antenna," in *Proc. Antennas Propag. Soc. Int. Symp.*, vol. 21, May 1983, pp. 63–66.
- [18] S. Gao, "Microstrip antenna elements and dual-polarized arrays for active integration," Ph.D. dissertation, Dept. Elect. Comput. Eng., Shanghai Univ., Shanghai, China, 1999.
- [19] S. Gao, L. Li, and P. Gardner, "Recent research developments in microwave theory & techniques," in *Proc. Dual-Polarized Antennas Wireless Commun. Radar Syst.*, B. Beker and Y. Chen, Eds. Kerala, India: Research Signpost, 2002, ch. 8, pp. 1–28.
- [20] K. Woelder and J. Granholm, "Cross-polarization and sidelobe suppression in dual linear polarization antenna arrays," *IEEE Trans. Antennas Propag.*, vol. 45, no. 12, pp. 1727–1740, Dec. 1997.
- [21] D. Guha, M. Biswas, and Y. M. M. Antar, "Microstrip patch antenna with defected ground structure for cross polarization suppression," *IEEE Antennas Wireless Propag. Lett.*, vol. 4, pp. 455–458, 2005.
- [22] C. Kumar, M. I. Pasha, and D. Guha, "Microstrip patch with nonproximal symmetric defected ground structure (DGS) for improved cross-polarization properties over principal radiation planes," *IEEE Antennas Wireless Propag. Lett.*, vol. 14, pp. 1412–1414, 2015.
- [23] D. M. Pozar and S. M. Duffy, "A dual-band circularly polarized aperture-coupled stacked microstrip antenna for global positioning satellite," *IEEE Trans. Antennas Propag.*, vol. 45, no. 11, pp. 1618–1625, Nov. 1997.
- [24] D. M. Pozar, "Microstrip antenna aperture-coupled to a microstripline," *Electron. Lett.*, vol. 21, no. 2, pp. 49–50, Jan. 1985.
- [25] K. F. Lee, K. M. Luk, and H. W. Lai, *Microstrip Patch Antennas*. London, U.K.: Imperial College Press, 2010.
- [26] X. H. Yang and L. Shafai, "Characteristics of aperture coupled microstrip antennas with various radiating patches and coupling apertures," *IEEE Trans. Antennas Propag.*, vol. 43, no. 1, pp. 72–78, Jan. 1995.
- [27] M. Yamazaki, E. T. Rahardjo, and M. Haneishi, "Construction of a slot-coupled planar antenna for dual polarisation," *Electron. Lett.*, vol. 30, no. 22, pp. 1814–1815, Oct. 1994.
- [28] A. A. Serra, P. Nepa, G. Manara, G. Tribellini, and S. Cioci, "A wide-band dual-polarized stacked patch antenna," *IEEE Antennas Wireless Propag. Lett.*, vol. 6, pp. 141–143, 2007.
- [29] D. M. Pozar and F. Croq, "Millimeter-wave design of wide-band aperture-coupled stacked microstrip antennas," *IEEE Trans. Antennas Propag.*, vol. 39, no. 12, pp. 1770–1776, Dec. 1991.
- [30] R. M. Lebrón, J. L. Salazar, C. Fulton, S. Duthoit, D. Schmidt, and R. Palmer, "A novel near-field robotic scanner for surface, RF and thermal characterization of millimeter-wave active phased array antenna," in *Proc. 5th Int. Symp. Phased Array Syst. Technol.*, Boston, MA, USA, Oct. 2016, pp. 1–6.
- [31] T. M. F. Elshafiey, "Full wave analysis of a ferrite cross-patch antenna," in *Proc. Loughborough Antennas Propag. Conf.*, Apr. 2007, pp. 197–200.
- [32] D. M. Pozar, *Microwave Engineering*, 4th ed. Hoboken, NJ, USA: Wiley, 2012.
- [33] N. A. Aboerwal, J. L. Salazar, and C. Fulton, "Current polarization impact on cross-polarization definitions for practical antenna elements," in *Proc. 5th Int. Symp. Phased Array Syst. Technol.*, Oct. 2016, pp. 1–5.



**José D. Díaz** (S'12) received the B.S. degree in electrical and computer engineering and a Curriculum Sequence in atmospheric sciences and meteorology from the University of Puerto Rico at Mayagüez, Mayagüez, Puerto Rico, in 2015. He is currently pursuing the Ph.D. degree in electrical and computer engineering with The University of Oklahoma (OU), Norman, OK, USA, where he is involved in high-performance antenna elements for phased-array radars.

He spent four years as an Undergraduate Research Assistant with the Collaborative Adaptive Sensing of the Atmosphere Laboratory, Mayagüez, PR, USA. Along with undergraduate studies, he had the opportunity to be an intern with the National Weather Service, Miami, FL, USA, where research on hail storms in the peninsula was being conducted. He was involved in research on electromagnetic scattering and wave propagation with the Earth Observing Laboratory, National Center for Atmospheric Research, Boulder, CO, USA. He became a Research Assistant with the Advanced Radar Research Center, The University of Oklahoma, in 2015, under the supervision of Dr. J. Salazar.



**Jorge L. Salazar-Cerreno** (S'00–M'12–SM'14) received the M.S. degree in electrical engineering from the University of Puerto Rico at Mayagüez, Mayagüez, Puerto Rico, in 2003, and the Ph.D. degree from the University of Massachusetts at Amherst, Amherst, MA, USA, in 2012.

He joined the Department of Electrical and Computer Engineering, University of Puerto Rico at Mayagüez, as an Adjunct Professor, in 2012. In 2012, he also joined the Department of Electrical and Computer Engineering, Advanced Radar Research Center, The University of Oklahoma, Norman, OK, USA, as a Research Scientist and then as an Assistant Professor. His current research interests include radar for microwave remote sensing, active phased-array radars, antenna design, T/R modules, and electromagnetic scattering and propagation.

Dr. Salazar is a member of the Tau Beta Pi Honor Society of the IEEE TRANSACTIONS ON GEOSCIENCE AND REMOTE SENSING, the IEEE TRANSACTIONS ON ANTENNAS AND PROPAGATION, and the IEEE TRANSACTIONS ON AEROSPACE AND ELECTRONIC SYSTEMS. He was a recipient of the National Center for Atmospheric Research Advanced Study Program Post-Doctoral Fellowship in 2012.



**Javier A. Ortiz** (S'10) received the B.Sc. degree in electrical engineering from the University of Puerto Rico at Mayagüez, Mayagüez, Puerto Rico, in 2013. He is currently pursuing the Ph.D. degree with The University of Oklahoma, Norman, OK, USA.

He was an Undergraduate Research Assistant on projects in electromagnetics with the University of Puerto Rico at Mayagüez. In 2012, he co-founded the IEEE MTT/GRS/APS Joint Chapter and was the President from 2012 to 2014. From 2013 to 2014, he was a Volunteer Laboratory Teaching Assistant and a Graduate Research Assistant with the University's Puerto Rico Weather Radar Network. He is currently a Graduate Research Assistant with the Advanced Radar Research Center, The University of Oklahoma. His current research interests include microstrip patch antennas, modal analysis and filtering, high-purity radiating element designs, and high-performance active phased-array antennas.



**Nafati A. Aboserwal** (S'13–M'16) received the B.S. degree in electrical engineering from Al-Mergib University, Al Khums, Libya, in 2002, and the M.S. and Ph.D. degrees in electrical engineering from Arizona State University, Tempe, AZ, USA, in 2012 and 2014, respectively.

In 2015, he joined the Department of Electrical and Computer Engineering, Advanced Radar Research Center, The University of Oklahoma, Norman, OK, USA, as a Post-Doctoral Research Scientist and then as an Anechoic Chamber Manager. His current research interests include the EM theory, computational electromagnetics, antennas, the diffraction theory, active high-performance phased-array antennas for weather radars, higher modes, surface-wave characteristics of printed antennas, and high-performance dual-polarized microstrip antenna elements with low cross polarization.

Dr. Aboserwal is a member of the IEEE TRANSACTIONS ON ANTENNAS AND PROPAGATION.



**Rodrigo M. Lebrón** (S'16) was born in Asuncion, Paraguay. He received the B.S. degree in mechatronics from the Universidad Nacional de Asunción, San Lorenzo, Paraguay, in 2012, and the M.S. degree in mechanical engineering from the Universidade Federal do Rio Grande do Sul, Porto Alegre, Brazil, in 2015. He is currently pursuing the Ph.D. degree in electrical and computer engineering with The University of Oklahoma, Norman, OK, USA.

He is currently a Graduate Research Assistant with the Advanced Radar Research Center, The

University of Oklahoma. His current research interests include design and development of automated systems for measurement, characterization, and calibration of phased-array antennas.



**Caleb Fulton** (S'05–M'11–SM'16) received the B.S. and Ph.D. degrees in electrical and computer engineering from Purdue University, West Lafayette, IN, USA, in 2006 and 2011, respectively.

He is currently an Assistant Professor in electrical and computer engineering with the Advanced Radar Research Center, The University of Oklahoma, Norman, OK, USA. He is currently involved in a number of digital phased-array research and development efforts for a variety of applications. His current research interests include antenna design, digital phased-array calibration and compensation for transceiver errors, calibration for high-quality polarimetric radar measurements, integration of low-complexity transceivers and high-power GaN devices, and advanced digital beamforming design considerations.

Dr. Fulton is a member of the IEEE Antennas and Propagation, Aerospace and Electronic Systems, and Microwave Theory and Techniques Societies. He also serves on the Education Committee of the IEEE Microwave Theory and Techniques Societies. He received the Purdue University Eaton Alumni Award for design excellence for his work on the Army Digital Array Radar Project in 2009, the Meritorious Paper Award for a summary of these efforts from the 2010 Government Microcircuit Applications and Critical Technologies Conference, and the 2015 DARPA Young Faculty Award for his ongoing digital phased-array research.



**Robert D. Palmer** (S'86–M'89–S'93–F'17) was born in Fort Benning, GA, USA, in 1962. He received the Ph.D. degree in electrical engineering from The University of Oklahoma (OU), Norman, OK, USA, in 1989.

From 1989 to 1991, he was a JSPS Post-Doctoral Fellow with the Radio Atmospheric Science Center, Kyoto University, Kyoto, Japan, where his major accomplishment was the development of novel interferometric radar techniques for studies of atmospheric turbulent layers. He was with the Physics and Astronomy Department, Clemson University, Clemson, SC, USA. From 1993 to 2004, he was with the Faculty of the Department of Electrical Engineering, University of Nebraska, Lincoln, NE, USA, where his interests broadened into areas including wireless communications, remote sensing, and pedagogy. Soon after moving to the School of Meteorology, OU, as the Tommy C. Craighead Chair in 2004, he established the interdisciplinary Advanced Radar Research Center (ARRC). He is currently the Executive Director of ARRC and the Associate Vice President for research in OU. He has published widely in the areas of radar remote sensing of the atmosphere, with an emphasis on generalized imaging problems, spatial filter design, and clutter mitigation using advanced array/signal processing techniques. His current research interests include the application of advanced radar signal processing techniques to observations of severe weather, particularly related to phased-array radars and other innovative system designs.

Dr. Palmer is a fellow of the American Meteorological Society. He was a recipient of several awards for both his teaching and research accomplishments.